CONF-880506--2

MODULAR HIGH-TEMPERATURE GAS-COOLED REACTOR SHORT TERM THERMAL RESPONSE TO FLOW AND REACTIVITY TRANSIENTS

CONF-880506--2

DE88 008387

John C. Cleveland

Oak Ridge National Laboratory
P. O. Box Y
Oak Ridge, Tennessee

Research sponsored by the U.S. Nuclear Regulatory Commission Office of Nuclear Reactor Regulation under Interagency Agreement DOE 0554-0554-A1 with the U.S. Department of Energy under contract DE-AC05-84OR21400 with the Martin Marietta Energy Systems, Inc.

ABSTRACT

The analyses reported here have been conducted at the Oak Ridge National Laboratory (ORNL) for the U.S. Nuclear Regulatory Commission's (NRC's) Division of Regulatory Applications of the Office of Nuclear Regulatory Research. The short-term thermal response of the Modular High-Temperature Gas-Cooled Reactor (MHTGR) is analyzed for a range of flow and reactivity transients. These include loss of forced circulation (LOFC) without scram, moisture ingress, spurious withdrawal of a control rod group, hypothetical large and rapid positive reactivity insertion, and a rapid core cooling event. The coupled heat transfer-neutron kinetics model is also described.

INTRODUCTION AND PURPOSE

The MHTGR is an advanced reactor concept being developed under a cooperative program involving the U.S. Department of Energy, the nuclear industry, and the utilities. The conceptual design is being reviewed by the NRC. As part of this review, ORNL has analyzed the short-term thermal response of the reactor for a range of flow and reactivity transients. Certain actions of the plant control and protection system have been assumed not to function to examine the response to extremely unlikely events.

This work has been performed to: (1) enable comparisons with results obtained by the industry design team, and (2) search for conditions which lead to more severe transients than previously identified. To the extent possible at this stage of NRC's review, the results presented are independent of the designer's effort. However, values for important parameters — temperature coefficients of reactivity, reactivity worth of moisture, moisture ingress rate, control rod worth, and neutron generation time — used in these analyses were obtained from the designer. Investigations of the accuracy of these parameters and their uncertainty are underway and, if necessary, additional analyses will be conducted.

For this examination, fuel temperatures below 1600°C are considered acceptable. Investigations of the validity of this as well as reviews of plans by the developer to further substantiate acceptable fission product retention in fuel at temperatures in this range are also underway.

Unless otherwise noted, end-of-equilibrium cycle temperature coefficients of reactivity were used since they are the least negative values reported.

SUMMARY DESCRIPTION OF THE MHTGR

The MHTGR nuclear steam supply is shown in Fig. 1. The design utilizes basic HTGR features of ceramic fuel, helium coolant and a graphite moderator. The coated fuel particles are compacted in a graphite matrix into fuel rods and loaded in hexagonal graphite blocks. Reactor heat is transferred by a once through steam generator to produce high-temperature, high-pressure steam. Table 1 summarizes major design parameters.

SUMMARY OF PLANT CONTROL AND PROTECTION SYSTEM

Several actions are designed into the plant control and protection systems to limit and/or to terminate off-normal events involving flow and reactivity changes. These are:

1. the neutron flux controller,

2. a control rod trip on each of the following signals:
   - high neutron flux to helium mass flow ratio (1.40),
   - high primary system pressure (7.00 MPa),
   - low primary system pressure (5.76 MPa),
   - high steam generator inlet helium temperature (746°C), and
   - high primary coolant moisture concentration (1000 ppmv),

3. insertion of reserve shutdown material on each of the following signals:
   - high neutron flux to circulator speed ratio (1.80 with 30 s time delay), and
   - high primary system pressure (7.00 MPa),

4. a manual trip by the operator.

The reserve shutdown material is released into the core if the control rods fail to trip when commanded, or when excessive water enters the core.

In the events analyzed here, certain or all of these functions are assumed not to occur.

MODEL DESCRIPTION

The modeling uses techniques developed at ORNL during the past 14 years for HTGR analyses. The techniques have produced results in good agreement with measured transient response of the Arbeitsgemeinschaft Versuchs Reaktor (AVR) and of the Fort St. Vrain (FSV) reactor. Comparisons with measured data have been performed for reactivity insertions up to ~10¢ at rates up to 2¢/s, as well as for flow reductions including complete loss of forced circulation, with natural convection flow only. While these reactivity insertions and insertion rates are small compared with some considered in this paper, the good agreement with measured response gives some confidence that the modeling techniques provide reasonable results.

IBM's Continuous System Modeling Program (CSMP) language was utilized for these analyses. CSMP is an application oriented language that accepts models expressed in the form of ordinary differential equations and/or analog block diagrams. Input to the computational model includes a geometrical description of the core and fuel, the axial flux profile, fuel and moderator thermal properties, delayed neutron parameters, neutron generation time, equilibrium Xe^{135} reactivity worth, Xe^{135} microscopic absorption cross section, core macroscopic fission cross section, total neutron flux, and fuel and moderator temperature coefficients of reactivity. The time dependence of the reactivity introduced by control rods or by moisture is also required as input.

The core neutronic response is determined by the point kinetics equations with six groups of delayed neutron precursors:

$$\frac{dP}{dt} = \frac{\rho - \beta_T}{\Lambda} P + \Sigma \lambda_i C_i \qquad i = 1, \ldots, 6$$

$$\frac{dC_i}{dt} = - \lambda_i C_i + \frac{\beta_i}{\Lambda} P$$

where the parameters have their usual definitions. The core reactivity at any time t is computed from

$$\rho = \Delta\rho_f + \Delta\rho_m + \Delta\rho_{Xe} + \Delta\rho_{\text{control rods}}$$

The reactivity changes due to fuel and moderator temperature changes are

$$\Delta\rho_f(t) = \int_{\overline{T}_{f,ref}}^{\overline{T}_f} \alpha_f(T)dT \qquad \text{and}$$

$$\Delta\rho_m(t) = \int_{\overline{T}_{m,ref}}^{\overline{T}_m} \alpha_m(T)dT$$

where the fuel and moderator temperature coefficients are considered to be temperature dependent and the nuclear average fuel and moderator temperatures are obtained by volume and importance (flux squared) weighting of nodal temperatures determined by the coupled heat transfer analyses.

Although the model assumes the Doppler coefficient to be associated with temperature changes in the entire fuel compact matrix, it is in reality associated with temperature changes in only the fuel particles. To ignore the particle time constant is conservative in computing power excursions resulting from reactivity insertions. Reference 1 develops approximate analytical solutions of the coupled neutron kinetics-heat transfer equations to compare the power and temperature response for a step reactivity insertion that would be predicted with a fuel compact model with that predicted by a fuel particle model when each is coupled with the neutron kinetics equations. Results show that because of the coupling between temperature feedback and power generation, the fuel compact model delays the effect of the temperature feedback resulting in higher predicted maximum power. However, the temperature increase predicted by a fuel compact model is representative of the increase which would be predicted by a particle model, provided the fuel temperature coefficient computed on the basis of particle temperature change is about the same as that computed on the basis of fuel compact temperature change.

The time dependent Xenon reactivity change, $\Delta\rho_{Xe}(t)$ is computed by

$$\Delta\rho_{Xe}(t) = \Delta\rho_{Xe}(t=0) * \left[\frac{X(t)}{X(0)} - 1\right]$$

The time dependent Xe^{135} concentration, $X(t)$, is computed from differential equations for I^{135} and Xe^{135} concentrations:

$$\frac{dI}{dt} = -\lambda_I I - \sigma_I \phi I + \gamma_I \Sigma_f \phi$$

$$\frac{dX}{dt} = -\lambda_X X - \sigma_X \phi X + \lambda_I I + \gamma_X \Sigma_f \phi$$

After the reactor is driven subcritical, either by temperature increase or by insertion of control material, the total power including the decay power contribution is computed as the output of a series of optimized lead-lag filters with prompt power as an input and with filter coefficients and time constants selected to match decay power generation following a step decrease in flux to zero.

To determine the steady state and transient fuel and moderator temperatures, a lumped node model of an average fuel/moderator column is employed. This column is modeled by 20 axial sections. The heat transfer model is appropriate for conditions in which the heat removal from an average region by intra-region conduction is negligible compared to the difference between the heat generation in that region and the heat removed by convection. For cases involving forced convection, the axial conduction is neglected because heat transfer by conduction in the solid in the axial direction is negligible compared to the heat conducted outward from the fuel through the moderator and taken up by the coolant gas. Therefore heat transfer in the solid is determined by a set of radial heat transfer calculations coupled axially by means of the flowing coolant gas. The core inlet flow rate and inlet temperature can be varied during the transient by input.

Each of the twenty axial sections of the average fuel/moderator column is modeled with three nodes. Two of these represent the fuel stick and one represents the moderator. Therefore, the transient thermal response is computed by 60 first order, non-linear, time dependent differential equations of the form

$$\frac{d\overline{T}_{f1}}{dt} = \frac{\dot{Q}_{f1}V_{f1}}{(Mc_p)_{f1}} + \frac{C_1}{(Mc_p)_{f1}}(\overline{T}_{f2} - \overline{T}_{f1})$$

$$\frac{d\overline{T}_{f2}}{dt} = \frac{\dot{Q}_{f2}V_{f2}}{(Mc_p)_{f2}} + \frac{C_1}{(Mc_p)_{f2}}(\overline{T}_{f1} - \overline{T}_{f2})$$

$$+ \frac{C_2}{(Mc_p)_{f2}}(\overline{T}_m - \overline{T}_{f2})$$

and

$$\frac{d\overline{T}_m}{dt} = \frac{Q_m V_m}{(Mc_p)_m} + \frac{C_2}{(Mc_p)_m}(\overline{T}_{f2} - \overline{T}_m)$$

$$+ \frac{C_3}{(Mc_p)_m}(\overline{T}_s - \overline{T}_m)$$

The conductances C1, C2 and C3 are derived so that terms C_1 $(\overline{T}_{f1} - \overline{T}_{f2})$, C_2 $(\overline{T}_{f2} - \overline{T}_m)$, and C_3 $(\overline{T}_m - \overline{T}_s)$ properly represent the heat flow between successive radial nodes at steady state. A shape factor to account for the triangular lattice of fuel and coolant channels based on Ref. 2 is used.

The gas temperature along the z axis in each of the twenty sections of the core is computed from the inlet temperature, T_{in}, to that axial section and the coolant channel surface temperature, T_s, in that axial section according to the "exponential approach" technique:

$$T_{gas}(z) = e^{-nz/L}\, T_{in} + (1 - e^{-nz/L})\, T_s$$

with

$$n \equiv \frac{hA}{WC_{p,he}} ,$$

and L is the length of the section.

This relation is the exact solution to the equation

$$W\, C_{p,he}\, dT_{gas}(z) = h\, [T_s - T_{gas}(z)]\, dA$$

where T_s is assumed constant along each axial section. This quasi-static approximation is practical due to the small energy storage in the helium relative to that in the core and due to the small transport time of helium through the core relative to the thermal time constant of the fuel. The gas outlet temperature from each axial section is

$$T_{out} = e^{-n} T_{in} + (1 - e^{-n})T_s$$

The surface temperature, T_s, in each axial section is derived from

$$C_3(\overline{T}_m - T_s) = hA\ (T_s - \overline{T}_{gas})$$

where

$$\overline{T}_{gas} = T_s + \frac{1}{n}(e^{-n} - 1)(T_s - T_{in})$$

Defining $\gamma_F \equiv \frac{hA}{C_3}$, gives

$$T_s = (\overline{T}_m + \gamma_F\overline{T}_{gas})/(1 + \gamma_F)$$

LOSS OF FORCED CIRCULATION

For this event, it is assumed that circulator power is lost with the reactor initially operating at full power conditions. It is also assumed that there is no reactor scram and the shutdown cooling system does not operate. For the time interval considered, heat losses from the core through the reactor vessel by conduction, convection, and radiation to the reactor cavity were neglected.

Figure 2 shows the computed response. The flow reduction due to circulator coastdown (beginning at t = 60 s) results in increasing core temperatures since the thermal power exceeds the rate of heat removal by convection. The reactivity due to the moderator heatup is positive because of the slightly positive moderator temperature coefficient at operating temperatures. However, the reactivity due to the fuel heatup is sufficiently negative to drive the reactor subcritical. The reactor reaches decay power levels after about 300 s. The Xe^{135} concentration increases because of the reduced xenon burnout rate causing additional negative reactivity.

The higher than normal core temperatures, and the increasing xenon poisoning will be sufficient to hold the reactor subcritical for several hours. This allows a long time to insert the control rods or reserve shutdown material. If this is done prior to recriticality, maximum fuel temperatures would remain below those for a loss of coolant accident (LOCA) because natural convection of helium would tend to keep the core somewhat cooler than for a LOCA.

The response predicted here is in general similar to that demonstrated by several LOFC without scram tests conducted at the AVR pebble bed gas-cooled reactor at Jülich, West Germany. Such tests demonstrated the safe response of that reactor including a period of recriticality during which the reactor stabilized at a low power level (Ref. 3).

MOISTURE INGRESS

Figure 3 shows the response to reactivity introduced from moisture entering the primary system through a ruptured steam generator tube. The neutron flux controller should attempt to maintain constant power by driving control rods into the core. Also the safety protection subsystem should trip the reactor on a high power-to-flow signal. As an investment protection, the reactor is also tripped when a high moisture level is sensed. None of these functions has been assumed to be implemented here. The ingress rate as provided by the designer is initially high as the ruptured tube's inventory is expelled reducing to a quasi-static leak rate in 1.5 s. It was assumed that steam passes through the core as a front and that no moisture (or H_2) collects in the core. The transport time of the moisture from the steam generator to the core is 5 s. The circulator speed was assumed to remain constant.

The spikes in the power response result from repeated passes through the core of the front of higher concentration of moisture. The initial power increase to 116% power is a result of the ramp insertion of 0.0612% (12.8¢) reactivity during the front's first pass through the core (which requires 0.3 s). The prompt jump approximation, $\phi/\phi_o = \beta(1 - \rho)/(\beta - \rho)$, for a step insertion of this amount of reactivity predicts a power increase to 114.5%. Beyond 60 s, the assumption of homogeneous mixing in the primary system results in a smoother power response. The setpoint for reactor trip on high primary coolant moisture concentration would be reached a few seconds into the transient. Only 12 kg of moisture need be uniformly distributed through the circulating helium to reach the scram setpoint. The high power-to-flow trip level of 1.4 is reached about 210 s after initiation of the leak.

CONTROL ROD GROUP WITHDRAWAL

Results are shown in Fig. 4 for a spurious control rod group withdrawal event. This event involves withdrawal over 260 s of the control rod group of highest worth (2.5% Δk) without action of the neutron flux controller. The rod group is assumed to be initially fully inserted. The withdrawal is assumed to begin at $t = 60$ s. The reactor is assumed to scram on a high power-to-flow signal. The power peaks at 157% of normal 83 s after accident initiation. The average fuel temperature increases only 57°C before beginning to decrease due to the scram.

HYPOTHETICAL LARGE AND RAPID POSITIVE REACTIVITY INSERTION

Results are shown in Fig. 5 for a hypothetical control rod ejection event (assumed to begin at t = 5 s). This hypothetical event assumes rapid ejection of the control rod of highest worth (1.1% Δk) in 1 s. The designers claim this to be a noncredible event since it would require failure of the vessel penetration housing as well as structures located above the housing. It is analyzed here to examine plant response to a hypothetical large and rapid reactivity insertion. Since the system would depressurize, convective heat removal was assumed to cease at the time of rod ejection. Results show a large power spike terminated by the negative fuel temperature coefficient with an increase in average fuel temperature to ~1000°C. The hottest fuel in the core would reach a considerably higher temperature due to power peaking in the fuel near the rod being ejected.

RAPID CORE COOLING

Results are shown in Fig. 6 for a rapid core cooling event. This hypothetical event assumes that startup procedures are violated and the reactor is brought to temperatures corresponding to hot full power operation without coolant flow. The circulators are then started and taken rapidly to full cooling capacity. This results in a rapid cooldown introducing positive reactivity due to the negative overall temperature coefficient. It is assumed that no scram occurs.

This event was examined because it is a hypothetical method of possibly introducing a large net reactivity (potentially greater than one dollar) which could cause a very rapid and large power excursion that might result in excessive fuel temperatures. The initial power level was taken to be 100 kW, and fuel and moderator temperatures corresponding to full power operation were assumed for initial conditions.

When the helium flow is started and the fuel and moderator begin to cool, the strongly negative fuel temperature coefficient contributes a positive reactivity component. The slightly positive moderator temperature coefficient at normal operating temperatures contributes a negative reactivity component. The net reactivity is positive, and the power begins to increase rapidly. Until the power reaches levels that cause significant heating of the core, the net reactivity continues to increase and approaches one dollar. However, heatup of the core in turn decreases the net reactivity through the temperature feedback. Although the power reaches a very high level [850 MW(t)] the total energy deposition is not sufficient to increase temperatures above the initial (normal) values. The final condition is a power of 350 MW(t), as expected.

In order to examine the response to a case involving a net reactivity greater than one dollar, a second rapid core cooling case was examined with both the fuel and moderator temperature coefficients arbitrarily decreased by $2.0 \times 10^{-5}/°C$. Temperatures for this case were quite similar to those shown in Fig. 6, although the power peaked at a higher level [1475 MW(t)].

CONCLUSIONS

Keeping in mind that the designer's values for temperature coefficients, neutron generation time, control rod worth, moisture ingress rate and reactivity worth of moisture were used, certain conclusions can be drawn. If further examinations show considerably different values or large uncertainties for these parameters, certain cases analyzed here should be re-examined.

For events analyzed here, inherent features of the MHTGR provide a high degree of safety. First, there is a large margin of ~500°C between the maximum fuel temperature in normal operation (~1100°C) and the temperature for onset of fuel failure (~1600°C). Second, the core's high heat capacity and low power density result in slow temperature changes. At full power, the heatup rate of the core with no cooling at all (neither active nor passive),* would be only about 2.7°C/s. At decay power levels, the heat-up rate with no cooling at all would be in the range of 1 to 5% of this value. Finally, the negative overall temperature coefficient of reactivity which is in the range of -2×10^{-5}/°C to -5×10^{-5}/°C, tends to reduce core power as core temperatures increase.

No events were identified which could lead to considerably more severe conditions than previously thought. The plant control and protection system scram setpoints should provide adequate protection for transients analyzed here. Some hypothetical events, if not terminated by reactor scram, could result in temperatures in excess of the 1600°C limit for onset of fuel failure. However these events involve combinations of low probability failures. Further, the 1600°C limit is for longer term heatup and may be overly conservative for short term excursions.

Specific conclusions are

1. Loss of forced circulation:

- Fuel temperatures should remain below 1600°C if control rods or the reserve shutdown material are inserted prior to recriticality. Several hours are available for this action to be performed.
- Tests at the AVR have shown safe response to a LOFC without scram, including a period of recriticality.

---

*This is hypothetical and for illustration only. Clearly, if the core were not cooled it would become subcritical due to the negative temperature feedback, and could not remain at full power.

2. Moisture ingress:

- The reactivity introduced by a single tube rupture does not result in a large excursion. The transient is fairly slow, and if a scram occurs on high moisture content or on high power-to-flow ratio excessive fuel temperatures will not be reached.

3. Control rod group withdrawal transients:

- Increases in average fuel and moderator temperatures are small if a scram occurs on a high power-to-flow signal.
- Insertion of control rods or reserve shutdown material is necessary to maintain fuel temperatures below 1600°C.

4. Hypothetical large and rapid positive reactivity insertion:

- The system should be designed to make events such as control rod ejection incredible.

5. Rapid core cooling event:

- Fuel temperatures remain well below 1600°C. In fact, fuel temperatures do not rise above normal operating levels.

REFERENCES

1. J. C. CLEVELAND, *Modular High-Temperature Gas-Cooled Reactor Short Term Thermal Response to Flow and Reactivity Transients*, ORNL/TM (in preparation).

2. J. C. CLEVELAND, *CORTAP: A Coupled Neutron Kinetics - Heat Transfer Computer Program for the Dynamic Simulation of the High-Temperature Gas-Cooled Reactor Core*, ORNL/NUREG/TM-39, January 1977.

3. K. J. KRUEGER and G. P. IVENS, Safety-Related Experiences with the AVR Reactor, Proceedings of a Specialist's Meeting on Safety and Accident Analyses for Gas-Cooled Reactors Sponsored by the International Atomic Energy Agency, Oak Ridge, Tennessee, May 1985, IAEA-TECDOC-358.

Table 1. Summary MHTGR design parameters

Thermal power	350 MW(t)
Steam conditions	538°C (1000°F) 163 atm (2400 psig)
Core exit helium temperature	687°C (1268°F)
Cold helium temperature	258°C (497°F)
Core power density	5.9 W/cm^3

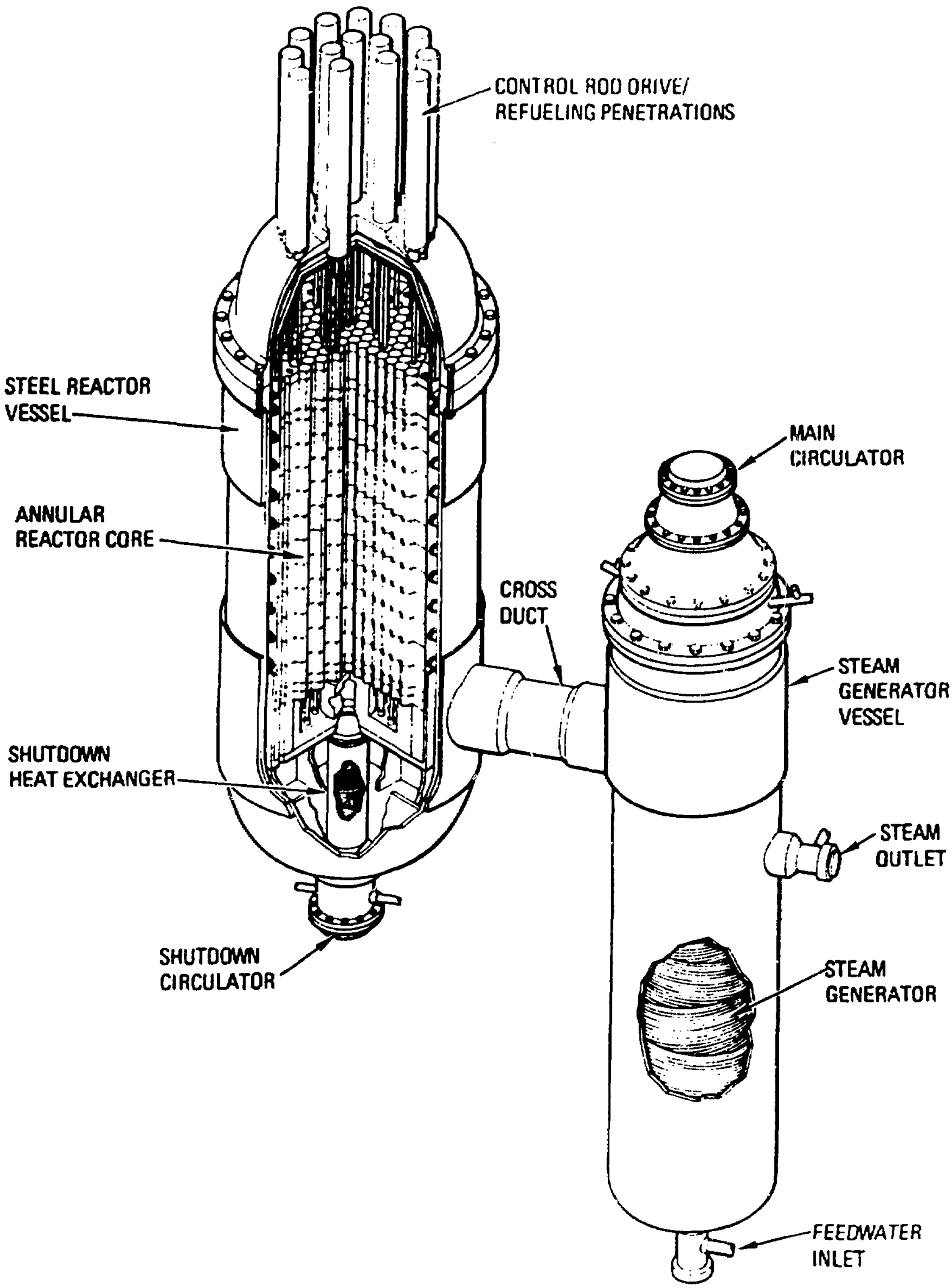

Figure 1. MHTGR nuclear steam supply

Fig. 2a. Temperature, power, and flux response during loss of forced circulation without scram.

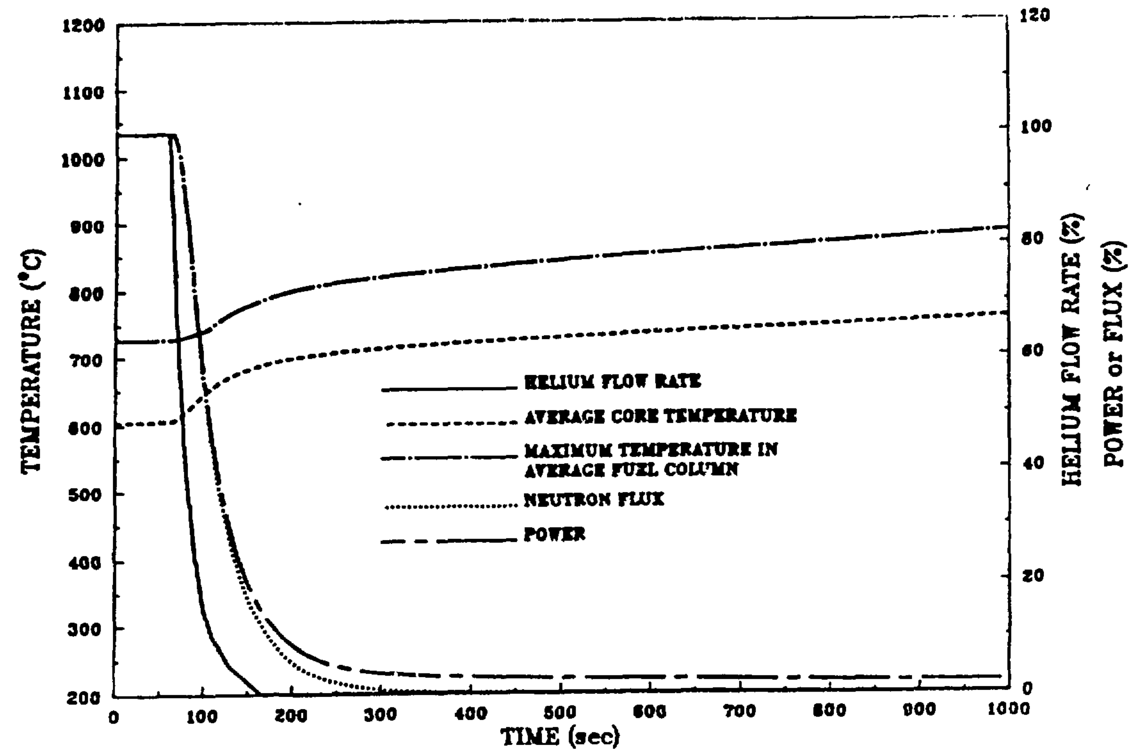

Fig. 2b. Reactivity response during loss of forced circulation without scram.

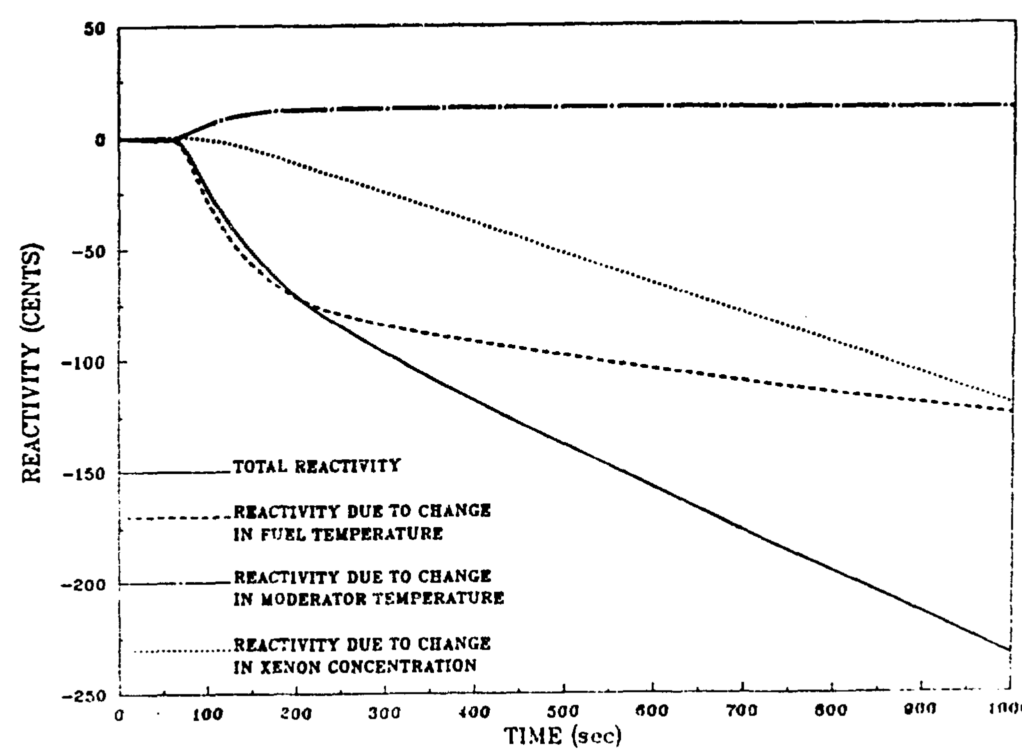

Fig. 3a. Temperature and power response during moisture ingress event.

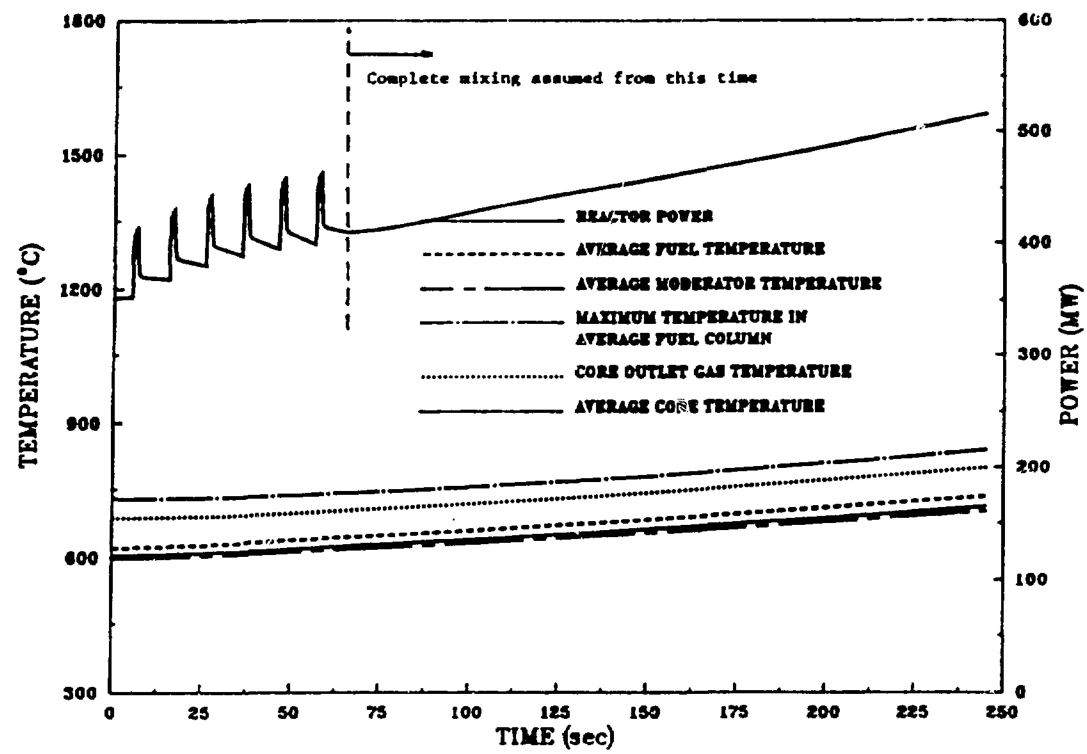

Fig. 3b. Reactivity response during moisture ingress event.

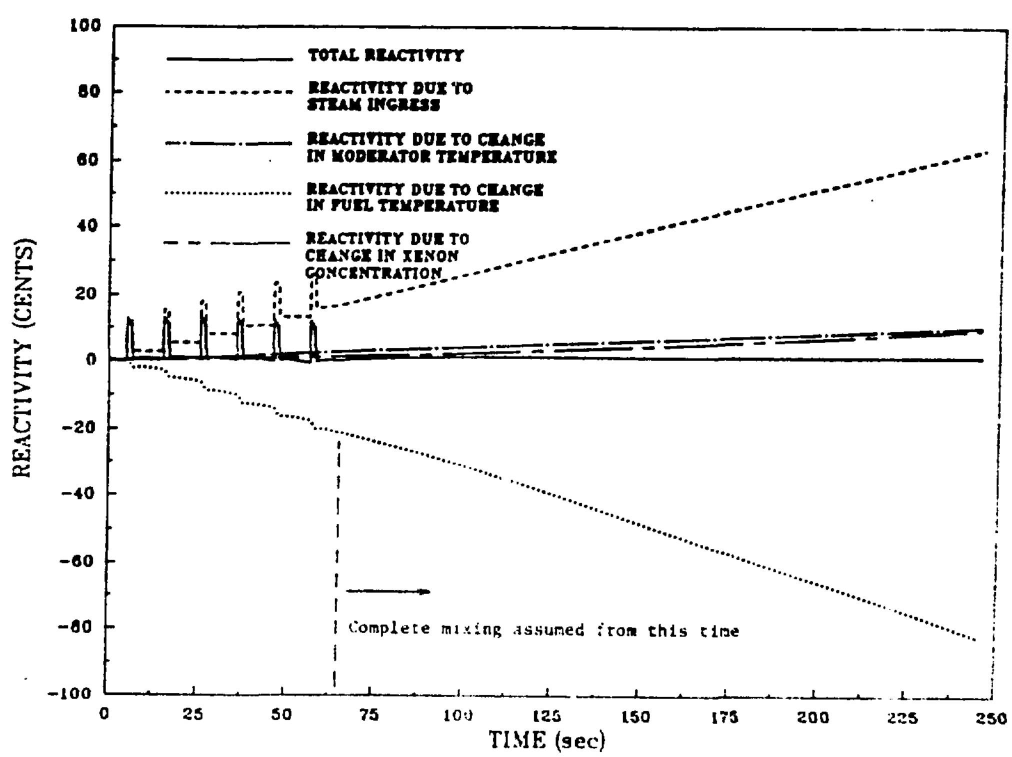

Fig. 4a. Temperature and power response during spurious control rod group withdrawal.

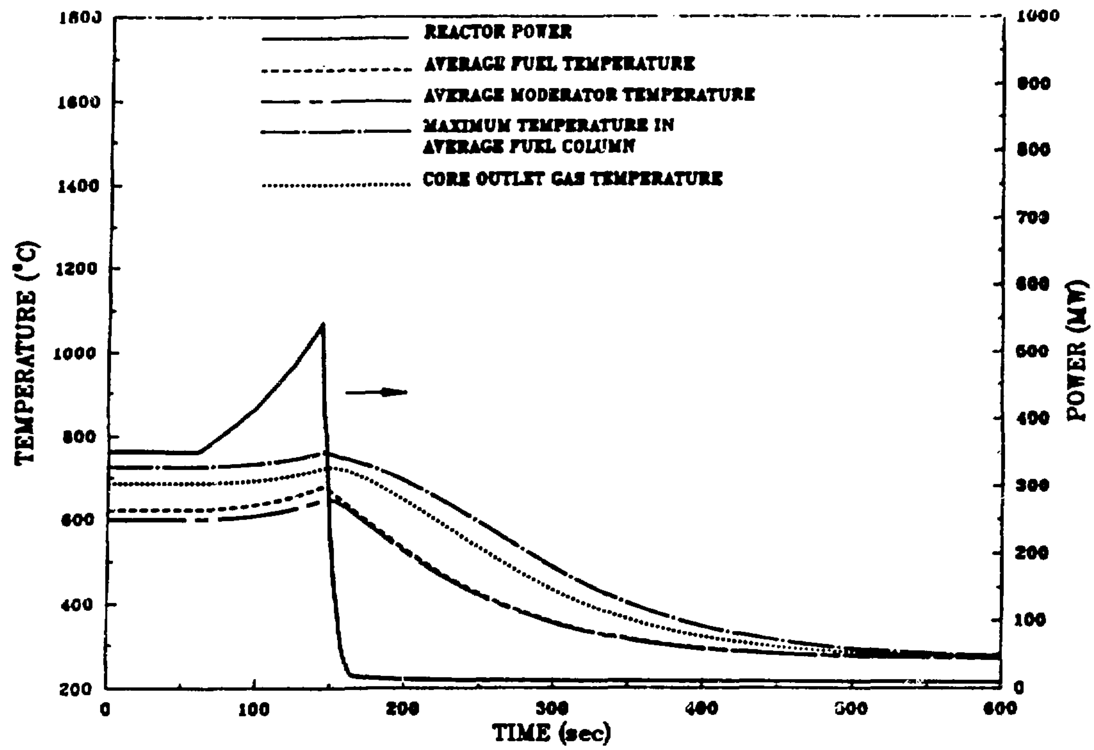

Fig. 4b. Reactivity response during spurious control rod group withdrawal.

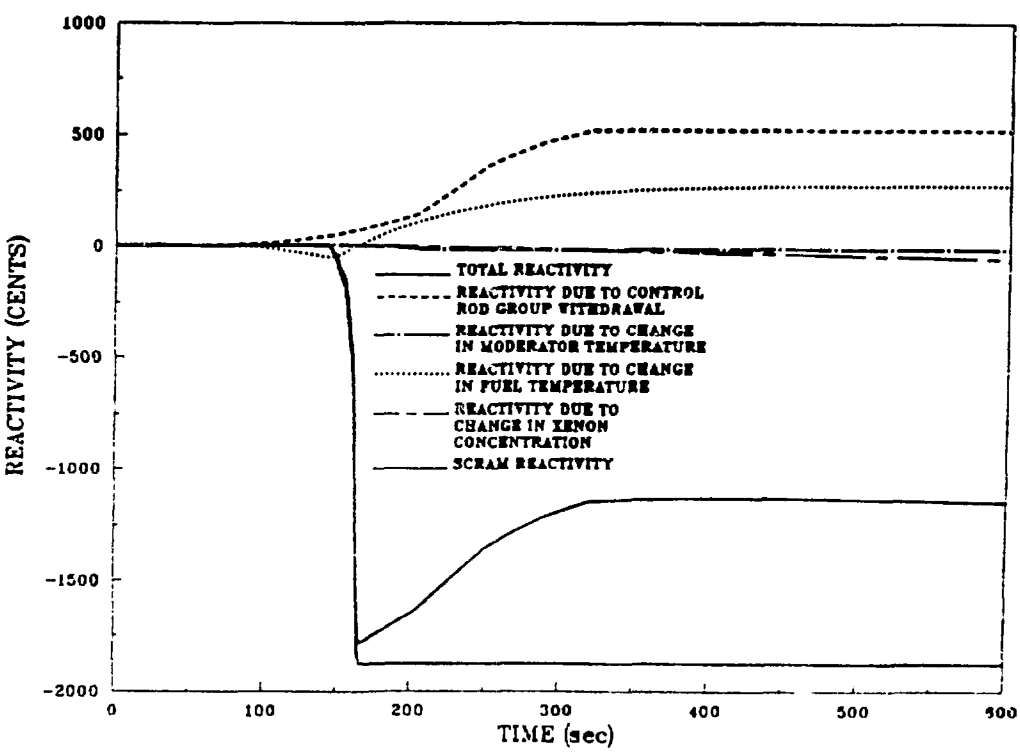

Fig. 5a. Temperature and power response during control rod ejection event.

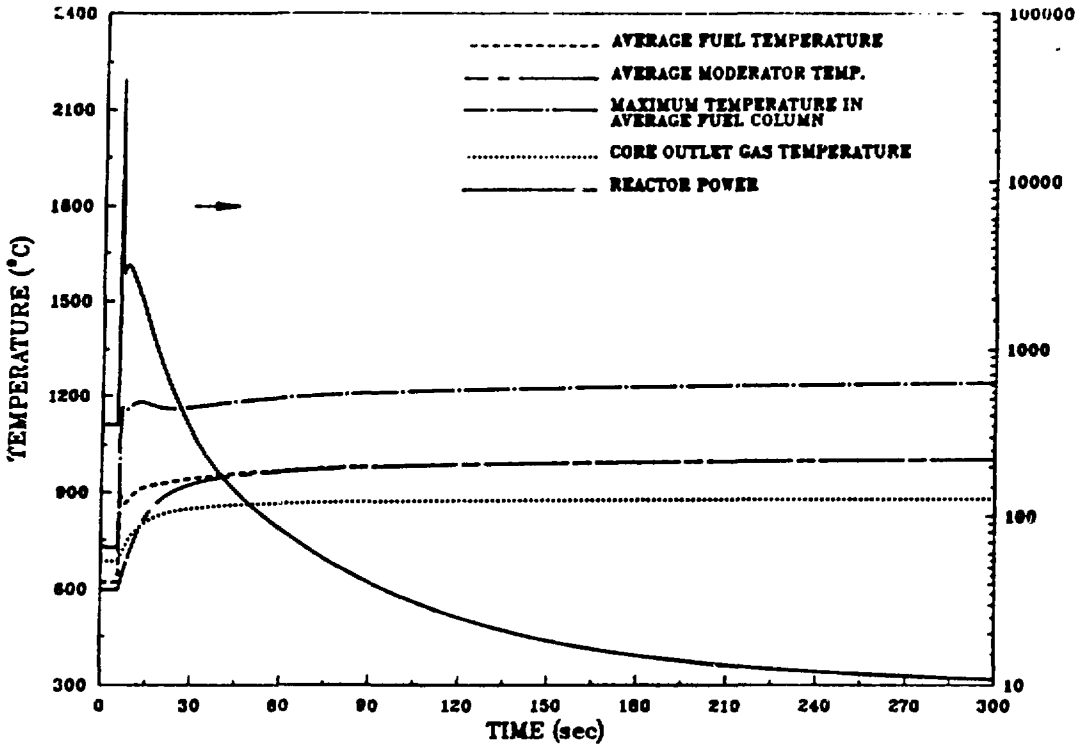

Fig. 5b. Reactivity response during control rod ejection event.

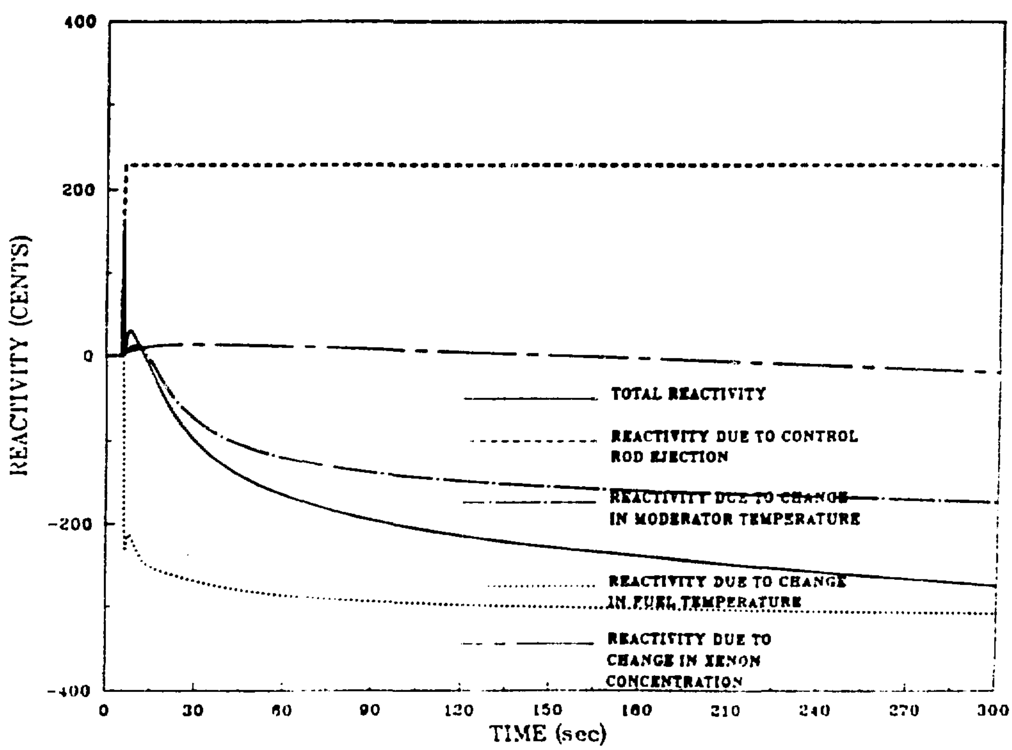

Fig. 6a. Temperature and power response during rapid cooling event.

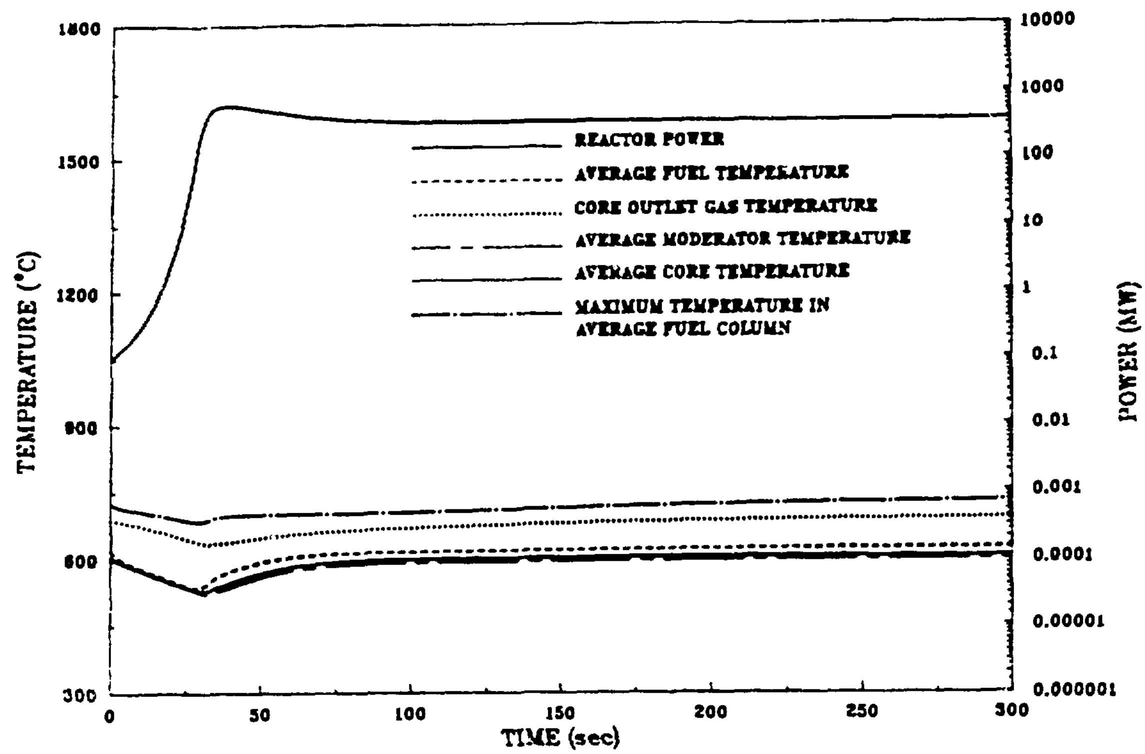

Fig. 6b. Reactivity response during rapid cooling event.